Robotica (2006) volume 24, pp. 595–602. © 2006 Cambridge University Press
doi:10.1017/S0263574706002669 Printed in the United Kingdom

A surface-shape recognition system mimicking human mechanism for tactile sensation

Masahiro Ohka*, Jyunichi Takayanagi**, Takuya Kawamura† and Yasunaga Mitsuya††

(Received in Final Form: December 16, 2005. First published online: February 28, 2006)

SUMMARY

Tactile sensing is advantageous for the acquisition of local, proximal information such as the contact condition between a finger and an object. This type of sensing, however, is not suited for recognizing an entire object that is easily recognized by vision. The objective of this paper is to ease the limitations experienced in tactile sensing by using both a neural model based on the human tactile sensation and a tactile-oriented associative memory model to enable a robot to recognize object contours. In the model, first the direction vectors belonging to segments of the object contour are obtained from a filtered tactile pattern of the simulated neurons' excitation. Second, the vectors are quantized by the chain-symbolizing method and stored for use in a memory matrix that accumulates matrix-products between the vector and its transposition. In the recalling process, complete vectors are remembered even if some input vector elements are missing. In the experiments, a robotic manipulator equipped with a tactile sensor traces five types of contours, these being a circle, a square, a triangle, a star, and a hexagon. After the robot recalls the complete contours, it is able to recognize a complete contour by just touching even a part of a contour.

KEYWORDS: Tactile sensor; Neuron model; Associative model; Contour recognition; Surface-shape.

I. INTRODUCTION

Tactile sensation is one of the important sensations for robotics because it has advantages that cannot be shared by other sensations such as vision or hearing.[1,2] Since it is not necessary to control conditions of lighting and reflection for tactile information processing and surface sensing, tactile sensation maintains a relatively high precision outside the laboratory because of insusceptibility to surroundings such as lighting conditions. In this work we focus on the advantages of tactile information processing and intend to establish a highly robust recognition system. In preceding papers, we presented a neuron model emulating a human mechanoreceptive unit for recognizing fine surface roughness on the basis of remarks[3–5] in the fields of neurophysics and psychophysics. This was done to apply the robust human recognition mechanism to robotics.[6]

In the present paper, as work subsequent to the above-mentioned papers, we intend finally to evolve or apply a robot equipped with the neuron model to environmental recognition performed with tactile and haptic sensing. Thus, we attempt to establish an entire model that emulates the tactile sensation mechanism, from tactile data acquisition with the mechnoreceptive unit to awareness as tactile sensation in the human brain, by combining the neuron model and a neural network model.

To date, many neural network models[7–10] have been presented to simulate human brain functions. We attempt to incorporate an associative memory model, which is a type of neural network model, into our recognition system, because tactile sensing is restricted to acquiring proximal information such as the contact condition between a finger and an object. The model requires a recall function to distinguish a whole shape from a portion of an object. This is the intrinsic asperity of tactile sensing, contrasting with visual sensing capable of acquiring a full image all at once. For example, we can recognize the position of a switch on a wall in a dark room, even if we touch just one part of the switch panel. In that process, associative information is retrieved using key information, and to date, this function has been formulated as the associative memory model.

To verify the present recognition system's surface-recognition capabilities, in this work we perform a series of experiments using a robotic manipulator equipped with the present recognition system and a tactile sensor. First, the robotic manipulator traces the edges of a fine stepped structure and estimates their directions. After verifying the precision level, we perform shape recognition of five fine relief-shaped contours, these being a circle, a square, a triangle, a star, and a hexagon.

II. OVERVIEW OF THE PRESENT RECOGNITION SYSTEM

As Fig. 1 shows, the present recognition system comprises the three modules described in the following chapters:

Corresponding author: M. Ohka. E-mail: ohka@is.nagoya-u.ac.jp
*Department of Complex Systems Science, Graduate School of Information Science, Nagoya University, Furo-cho, Chikusa-ku, Nagoya, 464-8601 (Japan).
** Toyota Motor Company.
†Gifu University.
†† Dept. of Micro System Engng, Graduate School of Engng, Nagoya University.

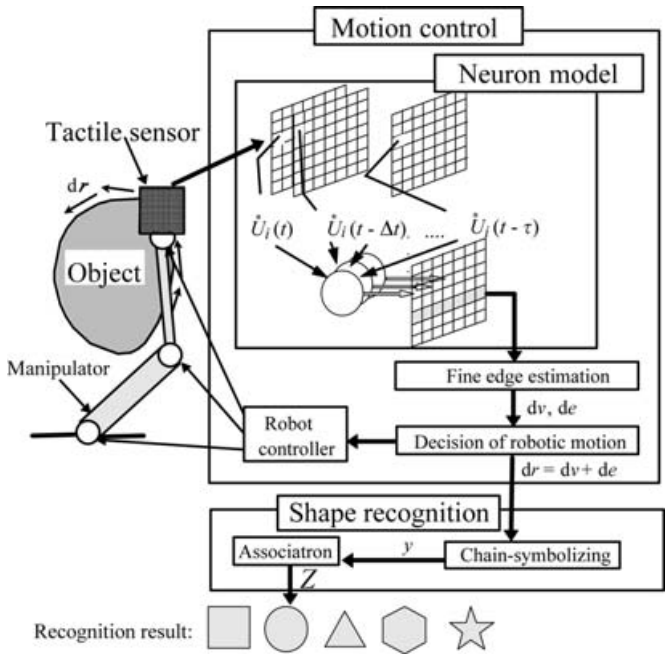

Fig. 1. Schematic view of the present tactile recognition system.

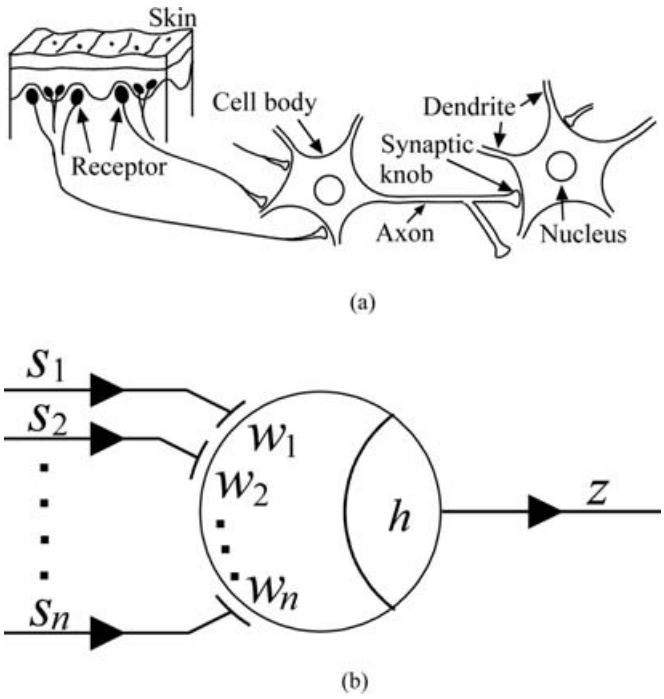

Fig. 2. Modeling of mechanoreceptive unit. (a) Schematic view of actual neurons. (b) Mathematical model.

the mechanoreceptive unit (neuron model) module, the motion control module, and the shape recognition module. In the present system, recognition of a contour shape is accomplished with robotic active motion and tactile sensing. That is, the system continues to recall the shape of contours scanned by the robot, while in the next step the robotic motion is decided and performed on the basis of tactile data obtained from active touches by the manipulator on the environment in a piecewise, robotic motion.

To recognize contours, the robotic motion of tracing an object edge is generated by the neuron model module and the motion control module. In the neuron model module, the position and height of a fine step are measured using the output of the simulated neuron mimicking the human tactile sensation. In the motion control module, the edge direction is estimated according to the output of the neurons. A robotic motion for tracing an object is then generated to align the center of the sensed surface with the edge of the step.

The edge directions obtained by the scanning motion are input to the associative memory model included in the shape recognition module one after the other. In the shape recognition module, the whole contour is recalled to the robot by a part of the contour data obtained during the edge tracing.

III. NEURON MODEL

In the preceding paper,[6] a mathematical model for the mechanoreceptive unit was formulated according to remarks[3–5] derived from human psychophysical experiments based on the McCulloch-Pitts model.[7] Figure 2 shows a neural network related to the tactile sensory system. When mechanical stimuli are applied to the surface of the skin, the mechanoreceptor accepts the stimulus and emits an electric signal. The signal is transmitted to a dendrite extending from a neuron through a synaptic connection. The arrival of the output signal from the mechanoreceptor effects a change in the membrane potential inside the neuron. If several signals from mechanoreceptors arrive almost simultaneously at the neuron, these signals are superimposed in the neuron and the summation of these signals changes the membrane potential. This effect is called *spatial summation* and is modeled first.

The neuron accepts n-signals $s_1, s_2, \ldots, s_n$ emitted from n-mechanoreceptors distributed in the skin (corresponding to n-elements of a tactile sensor in robotics). The weight of the synaptic connection between the i-th mechanoreceptor and the neuron is represented as w_i. Taking into account the spatial summation, the membrane potential, u is calculated as

$$u = \sum_{i=1}^{n} w_i s_i . \tag{1}$$

The mechanoreceptor seems to detect the time derivative of skin deformation. Since it is assumed that the mechanoreceptor detects the strain rate caused in the skin and that it emits signals proportional to the magnitude of the strain rate, instead of the strain rate emitted by the mechanoreceptor we designate displacement rate of the sensing element as s_i of Eq. (1) for the robotic tactile sensor. Namely, the output of the i-th sensing element s_i of Eq. (1) is calculated by the following expression,

$$s_i = a \left| \frac{dU_i}{dt} \right|, \tag{2}$$

where U_i is the displacement of the i-th sensing element and a is a coefficient.

https://doi.org/10.1017/S0263574706002669 Published online by Cambridge University Press

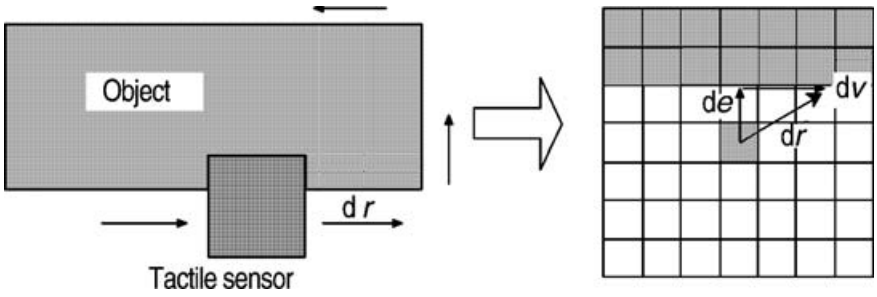

Fig. 3. Principle of edge tracing.

When an output signal emitted from the mechanoreceptor arrives at the neuron, a change occurs in the membrane potential. If the next signal arrives at the neuron before the change attenuates and vanishes, the next signal is superimposed on the residual of the preceding signal. This effect is called *time summation*, and is formulated as the convolution integral of $w_i(t-t')x_i\,(t')$ with respect to t' from the past to the present t if the weight of the synaptic connection between the i-th mechanoreceptor and the neuron is represented as $w_i(t')$ at time t'. Consequently, by incorporating the time summation into Eq. (1), the membrane potential u is calculated as

$$u = \sum_{i=1}^{n} \int_{-\infty}^{t} w_i(t-t')x_i(t')\,dt'. \tag{3}$$

The influence of a signal's arrival on the membrane potential decreases with time. This effect is expressed as a decrease in the synaptic potential $w_i(t)$. However, there are no available data on variation in the synaptic potential. In the present paper, it is assumed that $w_i(t)$ varies as a square wave; namely, it takes a constant value during 0 to τ sec, after which it takes 0.

$$w_i(t) = \begin{cases} 1, & 0 \le t < \tau \\ 0, & t < 0 \end{cases}. \tag{4}$$

It is known that neurons exhibit the threshold effect where the neuron emits an output if the membrane potential u, expressed as Eq. (3), exceeds a threshold h. The output is a pulse signal and the pulse density of the signal is proportional to the difference between membrane potential u and threshold h. The signal's pulse density is expressed as z, while the threshold function, $\phi(q)$ is designated to formulate the threshold effect. The pulse density, z, is given by

$$z = \phi(u-h) \tag{5}$$

$$\phi(q) = \begin{cases} q, & q \ge 0 \\ 0, & q < 0 \end{cases}. \tag{6}$$

IV. MOTION CONTROL MODULE

Ishikawa[11] presented an active sensing method in which an object's contour is acquired by moving a tactile sensor along the contour. The present method is based upon Ishikawa's method. In Ishikawa's method, the error vector $d\mathbf{e}$ defined as the difference between the center of the sensor and the edge is obtained and reduced to zero by means of feedback control.

Figure 3 shows the principle of edge tracing. The system specifies a direction of piecewise motion whenever the tactile sensor acquires a frame of tactile image data. The feedback control is performed by piecewise manipulator movement $d\mathbf{r}$. The manipulator movement $d\mathbf{r}$ is defined as the resultant directional vector of edge $d\mathbf{v}$ and error vector $d\mathbf{e}$:

$$d\mathbf{r} = d\mathbf{v} + d\mathbf{e}. \tag{7}$$

If the height of the edge is quite large, then it is easy to obtain the directional vector of edge $d\mathbf{v}$. For example, an edge can be easily estimated with filtered contact pressure distribution by a Laplacian filter in the case of a rather high step height. The present neuron model is effective for fine step heights measuring less than 200 μm. In the present neuron model, however, the edge precision falls as the manipulator approaches from direction $d\mathbf{r}$ to edge direction $d\mathbf{v}$ because the number of excited neurons decreases.

Thus, at one point the robot scans two perpendicular X- and Y-directions as shown in Fig. 4, and the unit vector of the edge direction is obtained according to the scanning results.

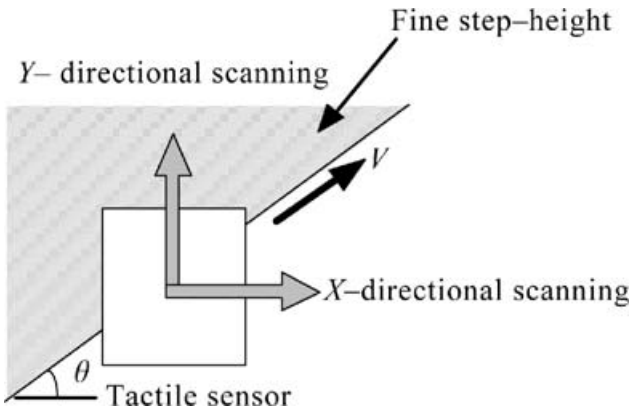

Fig. 4. Fine-edge direction estimation.

https://doi.org/10.1017/S0263574706002669 Published online by Cambridge University Press

The components of $d\mathbf{v}$ are calculated as follows:

$$\begin{cases} dv_x = \dfrac{\sum_{i=1}^{n}\sum_{j=1}^{n}(z_x)_{ij}\,V dt}{\sqrt{\sum_{i=1}^{n}\sum_{j=1}^{n}\left[(z_x)_{ij}^2+(z_y)_{ij}^2\right]}} \\ dv_y = \dfrac{\sum_{i=1}^{n}\sum_{j=1}^{n}(z_y)_{ij}\,V dt}{\sqrt{\sum_{i=1}^{n}\sum_{j=1}^{n}\left[(z_x)_{ij}^2+(z_y)_{ij}^2\right]}} \end{cases}, \tag{8}$$

where V is the scanning velocity at the edge, and $(z_x)_{ij}$ and $(z_y)_{ij}$ are the X- and Y-directional outputs of the neuron model, respectively. Subscripts i and j are row and column numbers of sensor cells, respectively. Since we intend to differentiate between going up and down the step, instead of $\phi(q)$ in Eq. (6) we use the three-value quantizing function $\Phi(q)$ defined as follows:

$$\Phi(q) = \begin{cases} +1 & (q > \varepsilon) \\ 0 & (-\varepsilon \le q \le \varepsilon), \\ -1 & (q < \varepsilon) \end{cases} \tag{9}$$

where ε is an appropriate threshold; we remove the sign of absolute norm from Eq. (2) and assume $h = 0$ in Eq. (5).

V. SHAPE RECOGNITION MODULE

V.1. Associative memory model

As described in the Introduction, since tactile sensing is restricted to acquiring proximal information such as the contact condition between a finger and an object, it requires a recalling function to be reminded of a whole shape from a portion of an object. We utilized the Associatron introduced by Nakano[8] to enable a robot to recall an entire contour from just one part of it. In the Associatron, information is represented by a hyper vector $\mathbf{x}$ comprising elements whose values are -1, 0, or $+1$:

$$\mathbf{x} = (x_1, x_2, \cdots, x_N), \tag{10}$$

where N is the dimension of the hyper vector.

In the memorizing process, tensor products produced by the vector and its transposition are stored in memory matrix $\mathbf{M}$:

$$\mathbf{M} = \mathbf{x}_{(1)}^T\mathbf{x}_{(1)} + \mathbf{x}_{(2)}^T\mathbf{x}_{(2)} + \cdots + \mathbf{x}_{(k)}^T\mathbf{x}_{(k)}, \tag{11}$$

where k is the number of stored items and the super subscript T indicates transposition.

The total number of stored items depends on the matrix dimension. The stored vectors should perpendicularly intersect each other to enhance the discriminating capability.

In the recalling process, a recalled vector $\mathbf{Z}$ is calculated from the matrix-vector product produced by the input vector $\mathbf{y}$ and the memory matrix $\mathbf{M}$:

$$\mathbf{Z} = \mathbf{\Phi}\{\mathbf{\Phi}(\mathbf{M})\mathbf{y}\}, \tag{12}$$

where $\mathbf{\Phi}(\mathrm{q})$ is defined in Eq. (9). According to this model, even if the input vector $\mathbf{y}$ is not perfect, the perfect output vector will be obtained.

V.2. Chain-symbolizing

To use the Associatron described in the previous section, the trajectory of the robotic manipulator needs to be transformed into the hyper-vector defined in Eq. (10). For example, for simplicity it is plausible that the manipulator's workspace is represented as a two-dimensional mesh, like a digital image, and that we put 1 or -1 as a coordinate on the manipulator's trajectory or 0 otherwise. However, if we select this quantizing method, the length of the hyper-vector will become impractically large; moreover, it will be difficult for it to correspond to the rotation and translation of a contour in the workspace.

Thus, we transform the manipulator trajectory to the hyper-vector form according to chain-symbolizing,[12,13] as shown in Fig. 5. First, we divide 2π into m divisions, that is, intervals $[2\pi(i-1)/m, 2\pi i/m]$, $(i = 1, 2, \ldots, m)$. Then, we count the direction frequency of $d\mathbf{r}$ within each interval and obtain the histogram shown in Fig. 5.

Next, the histogram is quantized to l levels by applying thresholds to obtain a hyper-vector of m $\times$ l elements. The value of the $i + m(j-1)$-th element of the vector is $+1$ if the frequency exceeds the threshold $d_j (j = 1, 2, \ldots, l)$:

$$x_{i+m(j-1)} = \begin{cases} +1, & f(i) \ge d_j \\ -1, & f(i) < d_j \end{cases}$$
$$(i = 1, 2, \ldots, m;\ j = 1, 2, \ldots, l) \tag{13}$$

where $f(i)$ is direction frequency of manipulator movement $d\mathbf{r}$.

According to the present chain codes, we can reduce the memory capacity demanded by the memory matrix. Additionally, the vector can easily correspond to the rotation and translation of a contour, since even if a contour translates in parallel, the histogram is invariant, thus the vector obtained from the translated contour can coincide with the vector of a not-translated contour.

If a contour rotates, the profile of the histogram shifts to the left or right. Likewise, the element number of the hyper-vector also shifts according to the rotational angle. Whenever cyclic replacements of the $i + m(j-1)$-th element to the $i + 1 + m(j-1)$-th and mj-th elements to the $1 + m(j-1)$-th are performed in turn from $i = 1$ to $i = m$ and from $j = 1$ to $j = l$, the hyper-vector obtained by the replacement is input to the Associatron to recall one of the memorized contours.

https://doi.org/10.1017/S0263574706002669 Published online by Cambridge University Press

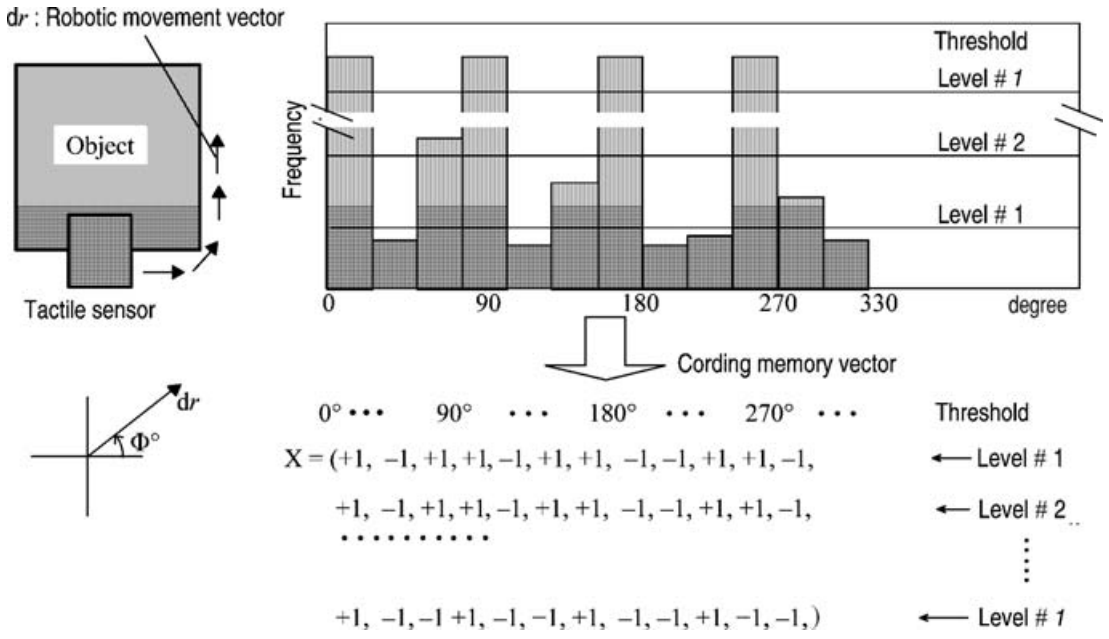

Fig. 5. Chain codes.

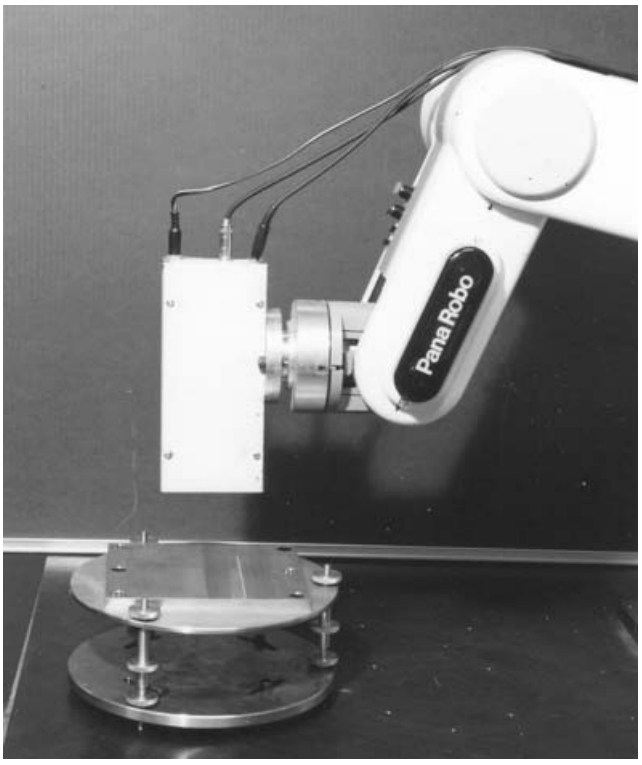

Fig. 6. Robotic manipulator with a tactile sensor.

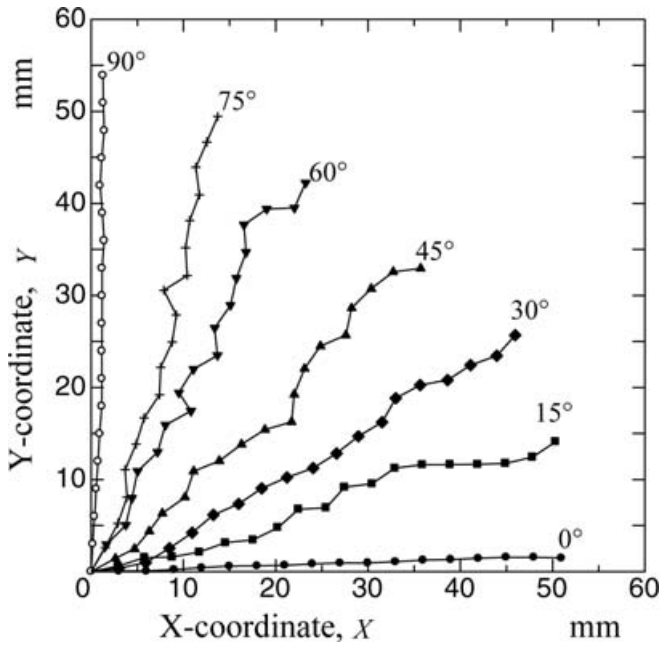

Fig. 7. Scanning precision for a fine step height.

VI. EXPERIMENTAL PROCEDURE

VI.1. Robotic manipulator equipped with a tactile sensor

Figure 6 shows a robotic manipulator with five degrees of freedom. The optical three-axis tactile sensor is mounted on the end of the manipulator.[14,15] The tactile sensor features an array comprising tactile elements capable of sensing a three-axis force. The size and pitch between two adjacent tactile elements of the array are 10×13 and 3 mm, respectively. Since we obtained a transform matrix from the force vector to the displacement vector, the sensor could measure the displacement of the sensing element's tip. In the present experiment, we measured the vertical displacement of 6×6 sensing elements located at the center of the array.

VI.2. Edge direction experiment

To verify the system's ability at detects edges of a fine step, we made a specimen having such a structure. The hatched region in Fig. 4 shows a fine convex portion. In this experiment, the robot traces the edge of the fine step height of $\delta = 50\,\mu$m along different edge directions $\theta = 0$, 15, 30, 45, 60, 75, and 90°.

https://doi.org/10.1017/S0263574706002669 Published online by Cambridge University Press

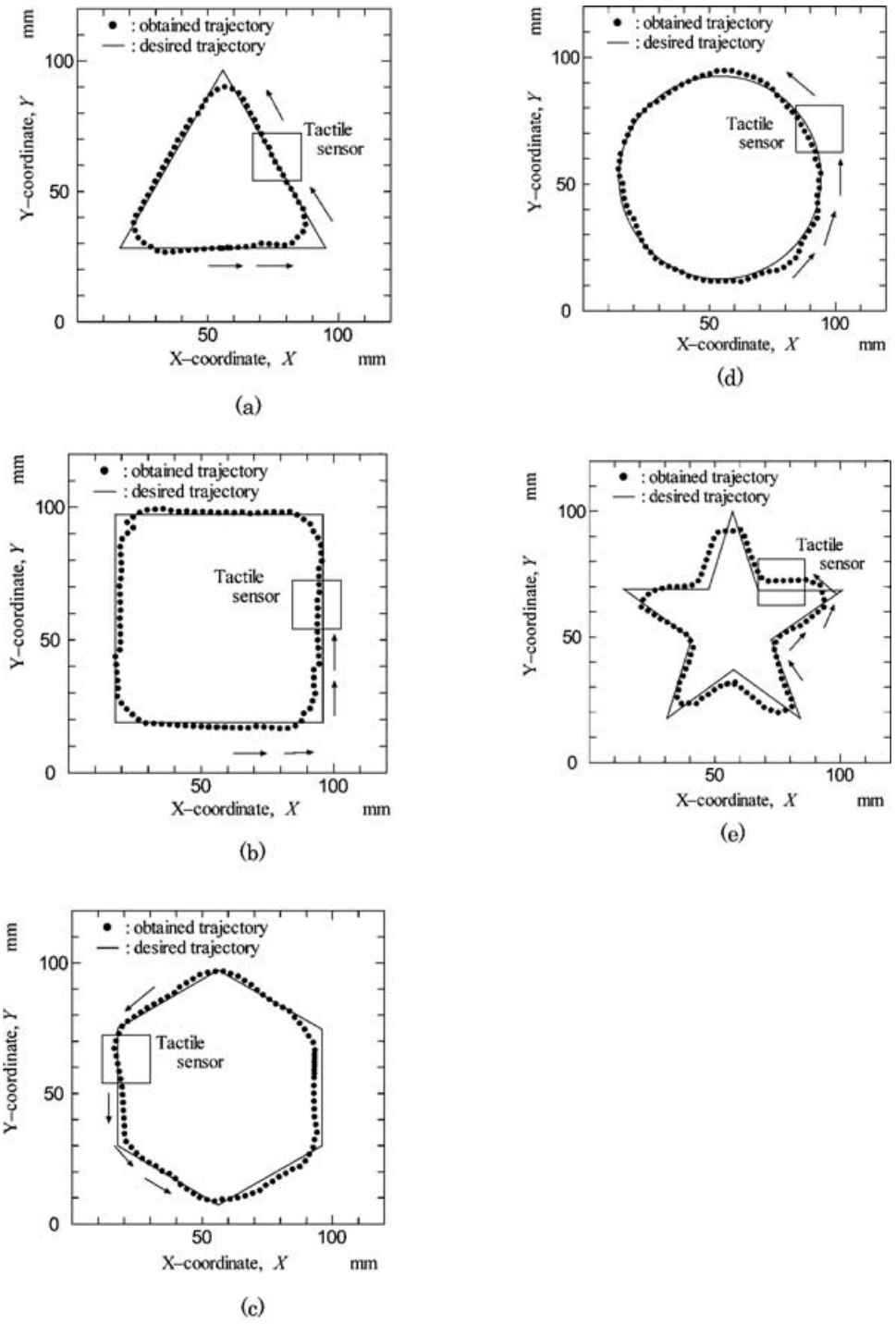

Fig. 8. Traceability of fine edges on figures. (a) Triangle. (b) Square. (c) Hexagon. (d) Circle. (e) Star.

VI.3. Shape recognition experiment

To verify ability of the associative memory, the robotic manipulator touched and explored fine step heights measuring $\delta = 200\ \mu$m, forming hexagonal, star-shaped, square, triangular, and circular patterns (diameter of a circumscribed circle of these figures: 90 mm). Motion control for the robotic manipulator was point-to-point (PTP). Each piecewise section of PTP motion was 3 mm, the same as the pitch between two sensing feelers on the tactile sensor. Hyper vectors **x** or **y** were obtained from a frame of the tactile image acquired in each piecewise section. As for contour recognition, the five specimen contours were first stored in the memory matrix. Then, Eq. (12) was calculated during tracing of the specimen to recall a stored contour. In this experiment, since number of angular divisions $m = 12$ and the number of threshold levels $l = 4$, number of elements per hyper-vector is 48.

VII. EXPERIMENTAL RESULTS AND DISCUSSION

VII.1 Edge direction experiment

In estimating the precision of fine edge tracings using the neuron model, Fig. 7 shows trajectories of the robot when it traces a fine step height $\delta = 50\ \mu$m. The ordinate and abscissa

https://doi.org/10.1017/S0263574706002669 Published online by Cambridge University Press

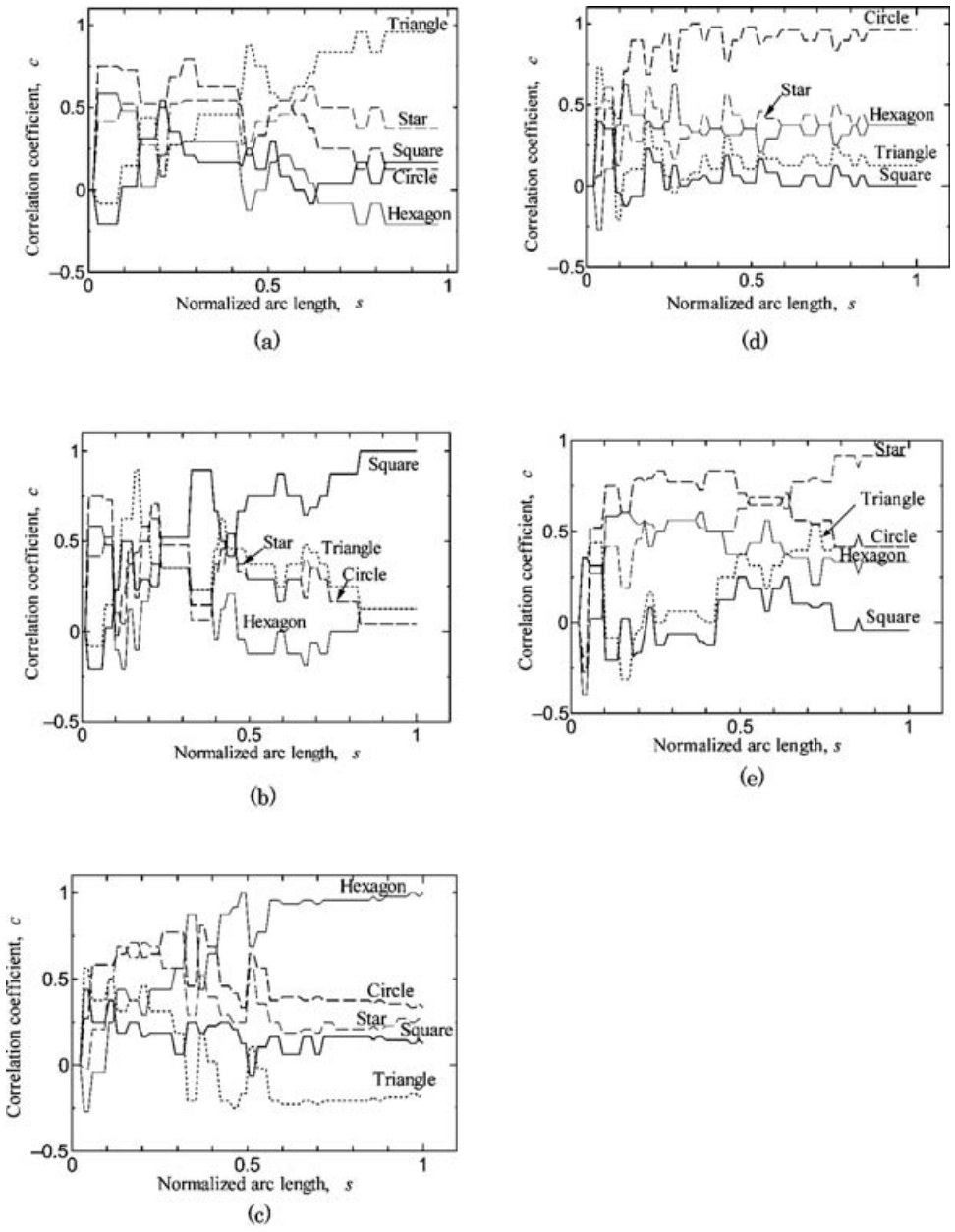

Fig. 9. Remembered results. (a) Triangle. (b) Square. (c) Hexagon. (d) Circle. (e) Star

of the graph are the X- and Y-coordinates, respectively. The values of correlation $|r|$ for five of the lines are within the range of 0.96 to 0.99. Therefore, the present system can discriminate a difference of 15° and trace linearly a fine edge, even if the step height is only 50 μm. However, since some vibrations are present, except for $\theta = 0$ and 90°, we chose 200 μm as the step height in the following sections.

VII.2. Contour tracing precision

Figure 8(a) ~ (e) shows the trajectories of five contours traced by the robot. In each figure, the ordinate and abscissa of the graph represent the X- and Y-coordinates, respectively. Each open square shows the dimension of sensing area. Therefore, despite their different shapes, the robot can trace the contours with satisfactory precision. If we examine the corner regions of each figure, we see that the difference between the obtained trajectory and desired trajectory becomes rather marked. Since the ratio of the arc length at the corners to the whole arc length is negligible, the disturbance at the corner does not affect recognition precision.

VII.3. Shape recognition experiment

The remembered result for the square is shown in Fig. 9(a) ~ (e). The abscissa of the figure denotes the position of the sensor's center using a normalized arc length, s, defined as l/L, where l and L are the arc length of the manipulator trajectory and the total manipulator trajectory, respectively. The ordinate of the figure is correlation c and is calculated as:

$$c = \frac{1}{N} \sum_{i=1}^{N} x_i Z_i, \tag{14}$$

where x_i and Z_i are components of the stored vector and output vector, respectively, and N is the number of

https://doi.org/10.1017/S0263574706002669 Published online by Cambridge University Press

components. The value of Eq. (14) becomes equal to unity if all components of vector **x** coincide completely with all components of vector **Z**. On the other hand, Eq. (14) becomes zero if all vector components are completely different. Correlation c indicates the degree of coincidence between two vectors.

When we examine the remembered result for the triangle, after $s = 0.61$ the value c for the triangle becomes the highest among all the figures. This signifies that the triangle is almost fully recalled if 61% of the remembering task is completed. From Fig. 9 (e), which shows the remembered result for the star, since we find that in the case of $s < 0.66$ the correlation for the star has almost the same value as the correlation for the circle, discrimination between the star and circle is the most difficult. However, other cases such as the circle and square are easily discriminated in the same manner as the triangle and hexagon. Therefore, this method is efficient for contour recognition using tactile sensing.

VIII. CONCLUSION

To ease the limitations that exist on tactile sensing, we have developed an edge-tracing system using a neuron model and an associative memory model. In the present system, the neuron model, emulating the human tactile sensation, is used for fine step-height measurement. First, the direction vectors belonging to segments of the object contour were obtained from an algorithm for fine step-height detection. Secondly, the vectors were quantized by a chain-symbolizing method and stored for use in a memory matrix that accumulates matrix products between the vector and its transposition.

To verify the present recognition system, we performed a series of experiments using a robotic manipulator equipped with a tactile sensor. In an edge detection experiment, the robot scanned a fine edge of $\delta = 50$ μm in different edge directions. The results indicated that the present system could discriminate difference to a margin of 15° and trace linearly the fine edge, even if the step height is just 50 μm.

In the recalling process, complete vectors were recalled even if the input vectors lacked some elements. In experiments, a robotic manipulator equipped with a tactile sensor traced five types of contours, including a circle, a square, a triangle, a star, and a hexagon. After the robot memorized the complete contours, it was able to recognize an entire contour even by touching just a part of a contour.

References

1. L. D. Harmon, "Automated Tactile Sensing," *Int. J. Robotics Research* **1–2**, 2–21 (1982).
2. H. R. Nicholls and M. H. Lee, "A Survey of Robot Tactile Sensing Technology," *Int. J. Robotic Research* **8–3**, 3–30 (1989).
3. T. Kawamura, M. Ohka, T. Miyaoka and Y. Mitsuya, "Measurement of Human Tactile Sensation Capability to Discriminate Fine Surface Textures Using Variable Step-height Presentation System," *Proc. of 5th IEEE Int. Workshop on Robot and Human Communication* (1996) pp. 274–279.
4. T. Miyaoka, T. Mano and M. Ohka, "Mechanisms of Fine-surface-texture Discrimination in Human Tactile Sensation," *The Journal of the Acoustical Society of America* **105–4**, 2485–2492 (1999).
5. T. Kawamura, M. Ohka, T. Miyaoka and Y. Mitsuya, "Human Tactile Sensation Capability to Discriminate Moving Fine Texture," *Proc. of IEEE Int. Workshop on Robot and Human Communication* (1998) pp. 555–561.
6. M. Ohka, T. Kawamura, T. Itahashi, J. Takayanagi, T. Miyaoka and Y. Mitsuya, "A Tactile Recognition System Mimicking Human Mechanism for Recognizing Surface Roughness," *JSME Int. J.*, **Series C, Vol. 48**, No. 2, 278–285 (2005).
7. W. McCulloch and W. Pitts, "A Logical Calculus of the Ideas Imminent in Nervous Activity," *Bulletin of Mathematical Biophysics* **7**, 115–133 (1943).
8. K. Nakano, "Associatron – A Model of Associative Models," *IEEE Trans SMC-2* (1972) pp. 381–388.
9. T. Kohonen, *Self-Organization and Associative Memory*, Second ed. (Springer-Verlag, New York, 1988).
10. B. Kosko, *Neural Networks and Fuzzy Systems* (Prentice Hall, New Jersey, 1992).
11. M. Ishikawa, "Active Sensing System Using Parallel Processing Circuits," *J. Robotics and Mechatronics* **5**, No. 1, 31–37 (1993).
12. K. S. Fu, R. C. Gonzalez and C. S. G. Lee, *Robotics – Control, Sensing, Vision, and Intelligence* 396–405 (McGraw-Hill, New York, 1987).
13. H. Ozaki, S. Waku, A. Mohri and M. Tanaka, "Pattern Recognition of Grasped Objects by Unit-Vector Distribution," *IEEE Trans. on Systems, Man, and Cybernetics*, **SMC-12-3**, 315–324 (1982).
14. M. Ohka, Y. Mitsuya, S. Takeuchi and O. Kamekawa, "A Three-axis Optical Tactile Sensor (FEM Contact Analyses and Sensing Experiments Using a Large-sized Tactile Sensor)," *Proc. 1995 IEEE Int. Conf. on Robotics and Automation* (1995) pp. 817–824.
15. M. Ohka, Y. Mitsuya, Y. Matsunaga and S. Takeuchi, "Sensing Characteristics of an Optical Three-axis Tactile Sensor Under Combine Loading", Robotica, **22**, 213–221 (2004).

https://doi.org/10.1017/S0263574706002669 Published online by Cambridge University Press